JOURNAL OF APPLIED POLYMER SCIENCE VOL. 12, PP. 353-372 (1968)

Correlation of Capillary Entrance Pressure Drops with Normal Stress Data*

H. L. LA NIEVE, III† and D. C. BOGUE, *Department of Chemical and Metallurgical Engineering, University of Tennessee, Knoxville, Tennessee*

Synopsis

The pressure loss at the entrance of a capillary tube was studied as a means of characterizing viscoelastic fluids. Measurements of four polymer solutions were made and correlated with an equation of the form

$$\Delta P_{end} = \alpha_2 H_{ch} \lambda_{ch}^{b_2} D^{b_2} + \alpha_3 H_{ch} \lambda_{ch}^{b_3} D^{b_3}$$

where D is the shear rate and where H_{ch} and λ_{ch} are a characteristic stress and a characteristic time, respectively, determined independently from viscosity and normal stress measurements. Various theoretical analyses of capillary entrance flow are also compared.

INTRODUCTION

The most fundamental experiments for measuring stress behavior in viscoelastic fluids are those in which the fluid elements have undergone constant shear rate histories for a very long time. These important *viscometric* flows[1] are found in the basic viscometric geometries: capillary tube, rotational cylinder, cone and plate, etc. On the other hand, many industrially important flows are accelerative (nonviscometric) and must be analyzed mathematically with a constitutive equation or be correlated empirically. The flow at the entrance of a capillary is this kind of flow. It is a particularly important one because of the wealth of data and experience from the capillary viscometer.

The measured pressure drop in a capillary viscometer is an overall one from the upstream reservoir to the downstream reservoir or from the upstream reservoir to a free jet. The frictional losses (viscous dissipation) include a loss upstream of the tube and inside the tube, due to the developing flow, a loss during developed flow in the tube, and a loss at the exit. There is also a kinetic energy (Bernoulli) effect if either reservoir is not large compared with the tube. These various effects plus possible elastic

* Paper presented at the symposium Mechanics of Rheologically Complex Fluids, Society of Petroleum Engineers of AIME, Houston, Texas, December 16, 1965.

† Present address: Celanese Research Company, Summit, New Jersey.

effects may be summarized in terms of a mechanical energy balance as follows:

$$\Delta P_{tot}/\rho = \Delta(\mathrm{KE}) + F_{upstrm} + F_{inside} + F_{dev} + F_{dwnstrm} + \underbrace{F_E + \Delta E}_{\Delta P_E/\rho} \quad (1)$$

kinetic energy; entrance friction; developed friction; exit friction; elastic effects

where F indicates irreversible dissipation, and Δ indicates differences between the exit and entrance regions. The symbol ρ is the fluid density. The quantity E is the elastic energy per unit mass and, in terms of the classic balance, is part of the internal energy of the fluid.[2,3] All effects excepting developed flow friction are classified as end effects and are denoted $\Delta P_{end}/\rho$.

For inelastic fluids (where $\Delta P_E/\rho = 0$) analyses are available for the dissipation in each of the sections indicated in eq. (1). For viscoelastic fluids no rigorous analysis exists, but if one assumes that the elastic effects may be added to the viscous effects (by no means certain), the elastic effects can be identified by difference and correlated experimentally. The analyses and procedures for the various terms will now be discussed in turn.

KINETIC ENERGY AND VISCOUS DISSIPATION EFFECTS

Kinetic Energy Effects

In a flow through a capillary from one stagnant reservoir to another the net change in kinetic energy is zero. However, at the entrance a pressure drop is required to impart a velocity to the fluid, although this pressure is recoverable in principle at the exit. However, the exit flow is not completely reversible, and the kinetic energy of the fluid is at least partially dissipated as friction, resulting in a net pressure loss of some fraction of the total kinetic energy. For a downstream reservoir this dissipation is accounted for by the term $F_{dwnstrm}$, and the kinetic energy term (ΔKE) is set equal to zero. For a downstream free jet the kinetic energy loss will be two velocity heads or somewhat less for non-Newtonian fluids.[4] Fortunately, in most polymer systems the flow rates are so low that the kinetic energy contribution (or downstream friction due to it) is negligible.

Developed Flow Dissipation

The pressure loss in developed flow is due entirely to viscous dissipation. This dissipation, denoted F_{dev} in eq. (1), has been quantitatively predicted by classical developments. The pressure drop may be related to the wall shear stress by a momentum balance, and the wall shear rate may be found for a general fluid in terms of the average velocity and capillary dimensions by the Mooney and Rabinowitsch relationship.[5,6] If a power law is as-

sumed to relate wall shear stress to wall shear rate in the capillary, the following equation will predict the pressure drop due to developed flow of a power-law fluid:

$$\Delta P_{dev} = \rho F_{dev} = (2L/R)H_{ch}\lambda_{ch}{}^{n}D^{n} \quad (2)$$

where D, the wall shear rate, is given by

$$D = (8V/d)(3n + 1)/4n$$

L is the capillary length, d and R are the capillary diameter and radius, respectively, and V is the mean fluid velocity. The lumped parameter $H_{ch}\lambda_{ch}{}^{n}$ and the parameter n are defined by the constitutive relation

$$T_{12} = H_{ch}\lambda_{ch}{}^{n}D^{n} \quad (3)$$

where T_{12} is the shear stress and D the characteristic shear rate (i.e., for developed capillary flow T_{12} is the wall shear stress and D the wall shear rate).

Dissipation Immediately Inside the Tube

Another end effect, which is appreciable at high flow rates but negligible at the flow rates of this investigation, is the excess viscous dissipation due to the development of the velocity profile near the entrance of the tube. The magnitude of this effect, denoted F_{inside} in the energy balance, eq. (1), has been predicted and measured for Newtonian fluids[7–11] and power law fluids.[8,12–14] Metzner and White[15] indicated from an analysis that the elastic effects due to profile development are a very small part of the measured elastic pressure drop.

Dissipation Outside the Capillary Tube

The viscous dissipation due to converging flow prior to the entrance and diverging flow at the exit of the capillary tube is significant for slow flows of very viscous fluids. These effects are designated F_{upstrm} and $F_{dwnstrm}$ in eq. (1).

Weissberg[16] showed for creeping Newtonian flow into or away from a thin orifice plate that the streamlines coincide with an oblate spheroidal coordinate axis. The pressure dissipated in the entrance was found to be

$$\Delta P_{ent} \equiv \rho F_{upstrm} = 3\eta Q/2R^{3} \quad (4)$$

where η is the Newtonian viscosity and Q the volumetric flow rate through the orifice. For creeping flow the exit flow into a large reservoir is identical with the entrance flow, and the total orifice pressure drop is therefore twice that at the entrance ($3\eta Q/R^{3}$). By a variational method Weissberg proved that the entrance and exit pressure loss for a flow into a finite length tube (rather than into a thin orifice plate) is less than 1.16 times the thin orifice result given above.

Tomita[17] presented an approximate solution for the energy loss due to converging flow into a capillary entrance for a viscous power-law fluid.

These results predict the energy loss in terms of the power-law fluid parameters with a larger loss for the more pseudoplastic fluids, i.e., lower n. The exit flow was not mentioned in Tomita's treatment.

ELASTIC EFFECTS

Qualitative Description

The elastic loss $\Delta P_E/\rho$ is made up of two terms: F_E, the dissipative loss due to any unusual flow patterns caused by the elasticity, and ΔE, the elastic internal energy acquired by the fluid between the ends of the viscometer. The lumping of the two terms is an admission of ignorance about where and in what way the elastic pressure loss takes place. It is certain, however, that F_E is not zero. In flow between two reservoirs one has $\Delta E = 0$ (complete relaxation), and thus the observed elastic pressure drop must be due to F_E. The most reasonable picture seems to be the following. Pressure energy is converted into elastic energy at the entrance, possibly with some irreversible loss during the process; this elastic energy is dissipated irreversibly at the exit as the fluid flows into the exit reservoir or jets into the atmosphere. One feels that perhaps some of the elastic energy could be recovered reversibly (as pressure). A useful but not conclusive experiment is to compare the pressure drop when a large exit reservoir is used with the pressure drop when a free jet at the exit is used, all other variables (tube diameter, tube length, and flow rate) being constant. Such experiments were performed with CMC–water and Separan–water solutions, and no difference was detected.[18] Since one expects irreversibility in the case of the free jet (there being no mechanism to harness the work), there apparently is complete irreversibility in the exit reservoir also. It is a tantalizing question whether the "appropriately" designed diverging exit used together with a fluid of "appropriately" high relaxation time would permit recovery of the elastic energy as pressure.

Analyses of Philippoff-Gaskins and Bagley

Philippoff and Gaskins[19] were the first to relate the excess viscoelastic pressure loss to the elastic property of the fluid. They found that a plot of total capillary pressure drop versus L/R at a constant shear rate is linear. The slope of this plot is equal to twice the developed flow wall shear stress, and the zero pressure intercept indicated that the end effects pressure loss could be treated as an effective additional length of tube (see Fig. 1). From an energy balance about the entrance this intercept on the abscissa was designated $e = n_c + S_R/2$, where e is the intercept, n_c is the tube length coefficient due to viscous end effects, and $S_R/2$ is the coefficient due to elastic effects (S_R is the "recoverable shear").

Bagley[20] showed that for fluids that followed "Hooke's law in shear," requiring $S_R = T_R/\mathrm{He}$, where He is an elastic modulus, the viscous and elastic effective lengths could be separated and individually evaluated

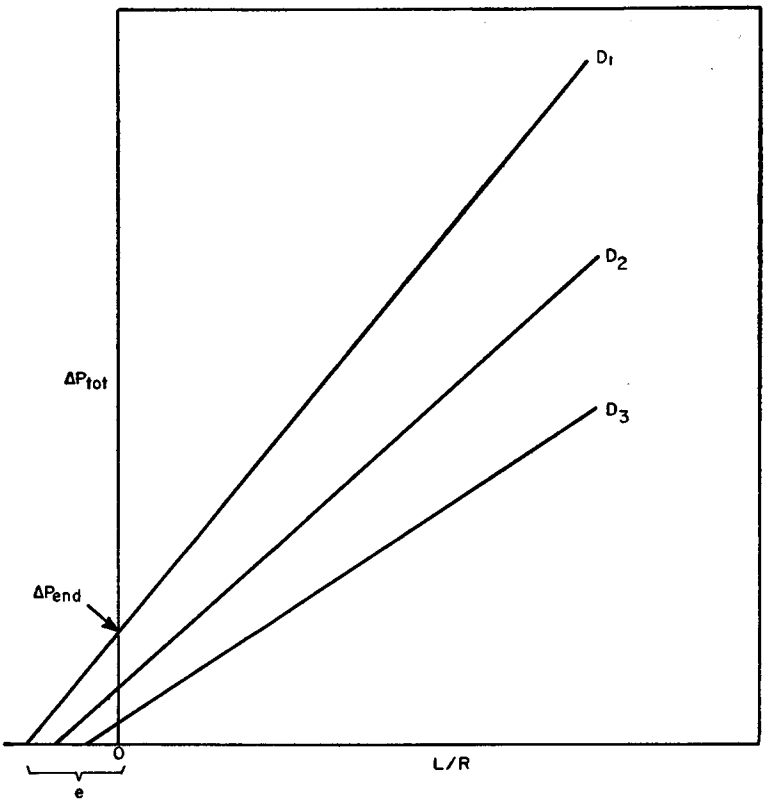

Fig. 1. Identification of pressure drop due to end flows.

from capillary data. For suitable fluids a plot of intercept e versus T_R should be linear, permitting the evaluation of n_c and S_R by this method. In terms of the end-effects pressure loss this method gives

$$\Delta P_{\text{end}} = 2n_c T_R^2/\text{He} \tag{5}$$

Analysis of Tomita

Tomita[21] developed a relationship for the elastic energy stored in the entrance flow. He used linear elastic theory modified by assuming a power relationship between strain and strain rate, to relate the elastic energy to the flow field. Streamlines were assumed for the entrance flow, and the energy equations were solved for elastic energy loss as a function of the material parameters and flow conditions. The viscous portion of the excess pressure loss was assumed equal to that of a purely viscous power-law fluid.

Second-Order Theory Analysis

The classic approach, consisting of solving the momentum balance equation in conjunction with a constitutive equation, was taken by La Nieve[18] for the viscoelastic entrance problem. After consideration of the

available constitutive theories[22] the Coleman-Noll second-order theory was selected, chiefly because it is the simplest theory that predicts normal stresses. Also important in the choice was the fact that this theory has been successfully used for describing mildly accelerating flows in a converging channel of small angle.[23]

A lucid derivation of the second-order Coleman-Noll equation is that of Coleman et al.[24] The second-order fluid is described as an incompressible simple fluid with a gradually fading memory. The short memory and Newtonian nature of the simple fluid theory limit its application to very low shear rates.

A rigorous solution of the momentum equation was not attempted. Rather, the streamlines were assumed along axes of three different coordinate systems, and the corresponding component of the momentum equation was integrated from infinitely far before the entrance up to the center of the entrance. This approach resulted in an equation of the entrance pressure drop in terms of the Coleman-Noll material constants and the velocity function along the streamlines. As a first approximation the Newtonian velocity profile was used.

Solutions were obtained for the entrance pressure drop assuming (*1*) flow along a coordinate axis of an oblate spheroidal coordinate system, (*2*) flow along rays to the center of the entrance in a spherical coordinate system (integration was carried out only to a distance equal to the capillary radius from the center of the entrance), and (*3*) flow along rays in a spherical coordinate system into a 114° cone. (The Newtonian analysis for radial flow into a cone of this angle predicts the same viscous pressure drop as was predicted by the oblate spheroidal analysis of Weissberg and was experimentally verified in this work.)

In these cases the resulting entrance pressure drop was a sum of a viscous term and an elastic term. For the oblate spheroidal case the viscous term was identical with the Newtonian viscous entrance loss of Weissberg.[16] The viscous term for the spherical coordinate case was identical to the Newtonian pressure loss in flow through a cone presented by Oka.[25]

The elastic terms were highly dependent on the flow lines assumed and the relative magnitudes of the two Coleman-Noll elastic material constants. The relative magnitudes of these constants are related to the secondary normal stresses in simple shear by

$$T_{22} - T_{33} = (\beta + 2\gamma)D^2 \tag{6}$$

where β and γ are the elastic material constants.

While Weissenberg's theory[26] requires that the secondary normal stress be zero (or $\beta = -2\gamma$), Markovitz and Brown[27,28] have presented data that indicate appreciable secondary normal stresses at low shear rates with relative values as high as $\beta = -4\gamma$.

The elastic portion of the pressure drop predicted by these analyses was much smaller in magnitude than has been reported for real viscoelastic

fluids. These predictions will be discussed in more detail after presentation of the experimental results.

DIMENSIONAL ANALYSIS

Despite the fact that many complex processes cannot be suitably treated analytically, much can be learned about them through dimensional analysis. Such a method will be applied to the viscoelastic end effects problem.

By putting into dimensionless form the equation of motion together with a general integral constitutive theory Bogue and Doughty[22] found that only two dimensionless parameters were necessary to characterize a flow field for a given viscoelastic material.

The dimensionless pressure drop due to end effects can be written as a function of these parameters along with some dimensionless material parameters as

$$\frac{\Delta P_{\text{end}}}{\rho V_{\text{ch}}^2} = \Phi\left[\frac{H_{\text{ch}}}{\rho V_{\text{ch}}^2}, \frac{\lambda_{\text{ch}} V_{\text{ch}}}{L_{\text{ch}}}, \text{dimensionless material parameters}\right] \quad (7)$$

where H_{ch} is a characteristic stress, λ_{ch} a characteristic time, V_{ch} a characteristic velocity, and L_{ch} a characteristic length. H_{ch} and λ_{ch} are material constants.

If the assumption is made that the function Φ may be represented by a general power series, the following equation should give the dimensionless entrance pressure drop:

$$\frac{\Delta P_{\text{end}}}{\rho V_{\text{ch}}^2} = \alpha_1 (H_{\text{ch}}/\rho V_{\text{ch}}^2)^{a_1}(\lambda_{\text{ch}} V_{\text{ch}}/L_{\text{ch}})^{b_1} + \alpha_2 (H_{\text{ch}}/\rho V_{\text{ch}}^2)^{a_2} \times (\lambda_{\text{ch}} V_{\text{ch}}/L_{\text{ch}})^{b_2} + \ldots \quad (8)$$

where $\alpha_1, \alpha_2, \ldots, \alpha_n$, $a_1, a_2, \ldots, a_n$ and $b_1, b_2, \ldots, b_n$ may be functions of dimensionless material parameters.

This equation will now be examined in the light of some physical facts.

(*1*) For large Reynolds numbers ($H_{\text{ch}}\lambda_{\text{ch}}/L_{\text{ch}} V_{\text{ch}}\rho \to 0$), the pressure drop is determined by the Bernoulli effect, which is of the form $\Delta P_{\text{end}}/\rho V_{\text{ch}}^2 = \alpha_1$. Therefore, a_1 and b_1 must be zero, along with $\alpha_2, \alpha_3, \ldots$.

(*2*) For Newtonian fluids in creeping flow ($H_{\text{ch}}\lambda_{\text{ch}}/L_{\text{ch}} V_{\text{ch}}\rho$ very large) $\Delta P_{\text{end}}/\rho V_{\text{ch}}^2$ depends only on a term involving the Reynolds number, $H_{\text{ch}}\lambda_{\text{ch}}/L_{\text{ch}} V_{\text{ch}}\rho$. For this situation the constants in eq. (8) must be

$$\alpha_1 = 0, \quad a_2 = b_2 = 1, \quad \alpha_2 = \text{finite}, \quad \alpha_3 = \alpha_4 = \ldots = 0$$

(*3*) For second-order fluids in creeping flow the analysis of this paper indicates that $\Delta P_{\text{end}}/\rho V_{\text{ch}}^2$ depends on two dimensionless terms, $H_{\text{ch}}\lambda_{\text{ch}}/L_{\text{ch}} V_{\text{ch}}\rho$ and $H_{\text{ch}}\lambda_{\text{ch}}^2/L_{\text{ch}}^2\rho$. The constants in this case must be

$$\alpha_1 = 0, \quad a_2 = b_2 = 1, \quad \alpha_2 = \text{finite},$$
$$a_3 = 1, \quad b_3 = 2, \quad \alpha_3 = \text{finite}, \quad \alpha_4 = \alpha_5 = \ldots = 0$$

(4) Experimental evidence indicates that in creeping flow ΔP_{end} depends only on the ratio V_{ch}/L_{ch} and not on either separately.[19,21,29,30] Solving eq. (8) for ΔP_{end} in creeping flow, where $\alpha_1 = 0$, gives

$$\Delta P_{end} = \alpha_2(H_{ch}/\rho V_{ch}^2)^{a_2}\rho V_{ch}^2(\lambda_{ch}V_{ch}/L_{ch})^{b_2} + \ldots \quad (9)$$

The restriction that ΔP_{end} must depend on the ratio V_{ch}/L_{ch} and not on either separately requires that $a_2 = a_3 = a_4 = \ldots = 1$, and eq. (9) reduces to

$$\Delta P_{end} = H_{ch}[\alpha_2(\lambda_{ch}V_{ch}/L_{ch})^{b_2} + \alpha_3(\lambda_{ch}V_{ch}/L_{ch})^{b_3} + \ldots] \quad (10)$$

Equation (10) should be a general expression for the pressure drop due to end effects for creeping flow subject to the restraint that the pressure drop is a function of V_{ch}/L_{ch} but neither separately. Any theory that predicts this pressure drop should then at least reduce to the form of this equation. Although the form is so general that the requirement that theories fit this form may not eliminate many incorrect theories, this form should prove useful in comparing the theories with one another.

COMPARISON OF ANALYSES

Equation (10) presents an ideal form for comparing the various analyses.

In order to simplify nomenclature, the characteristic parameters will be specified. The characteristic velocity and length will be chosen so that V_{ch}/L_{ch} is simply the wall shear rate in the capillary, denoted D. The characteristic stress H_{ch} and the characteristic time λ_{ch} will be chosen to be those defined by the following empirical power-law relationships:

$$T_{12} = H_{ch}\lambda_{ch}^{n}D^{n} \quad (11)$$

$$T_{11} - T_{22} = H_{ch}\lambda_{ch}^{2m}D^{2m} \quad (12)$$

where $T_{11} - T_{22}$ is the principal normal stress difference and D is the shear rate.

The specification of these parameters does not restrict the applicability of eq. (10) but does specify the values of the functions α_2, α_3, ..., and b_2, b_3, ...

In terms of the specified parameters eq. (10) becomes

$$\Delta P_{end} = \alpha_2 H_{ch}\lambda_{ch}^{b_2}D^{b_2} + \alpha_3 H_{ch}\lambda_{ch}^{b_3}D^{b_3} + \ldots \quad (13)$$

The analyses of the viscoelastic entrance pressure drop were arranged in the form of this equation and are presented for comparison in Table I. To fit Bagley's graphical method, represented by eq. (5), to this form, it was necessary to assume a power-law relationship between stress and shear rate. The elastic modulus He then becomes equal to the characteristic stress. To compare Tomita's analysis, it was necessary to substitute material parameters measured in shearing flow for his linear strain parameters. Tomita suggests that, although not rigorous, this appears to be the best way of evaluating these parameters.[31]

TABLE I
Comparison of the Measured End-Effects Pressure Loss with the Predictions of the Various Analyses

	$\Delta P_{end} = \alpha_2 H_{ch}\lambda_{ch}^{b_2} D^{b_2} + \alpha_3 H_{ch}\lambda_{ch}^{b_3} D^{b_3} + \ldots$				$\alpha_4,$
	α_2	b_2	α_3	b_3	$\alpha_5 \ldots$
Bagley analysis	$2n_c$ (evaluated empirically)	n	1	$2n$	0
Tomita analysis[a]	$K_V(n')$	n'	$K_E(n,'m')$	$2m'$	0
Second-order analyses					
A. Oblate spheroidal	$3\pi/4$[b]	1[b]	$-3(\beta + 4\gamma)/32\gamma$	2	0
B. Radial, plane entrance	1	1	$+ (24\beta + 28.5\gamma)/32\gamma$	2	0
C. Radial, 114° cone	2.3	1	$0.31(6.1\beta + 6.25\gamma)/\gamma$	2	0

[a] Prime indicates Tomita's material parameters, which differ from those of this paper.
[b] Identical with results from Weissberg's viscous analysis.

EXPERIMENTAL

The total capillary pressure loss was measured as a function of flow rate and capillary length-to-radius ratio by means of the apparatus shown in Figure 2. Four capillaries with length-to-radius ratio ranging between 5 and 200 were used. To ensure constant radius, glass tubing of radius

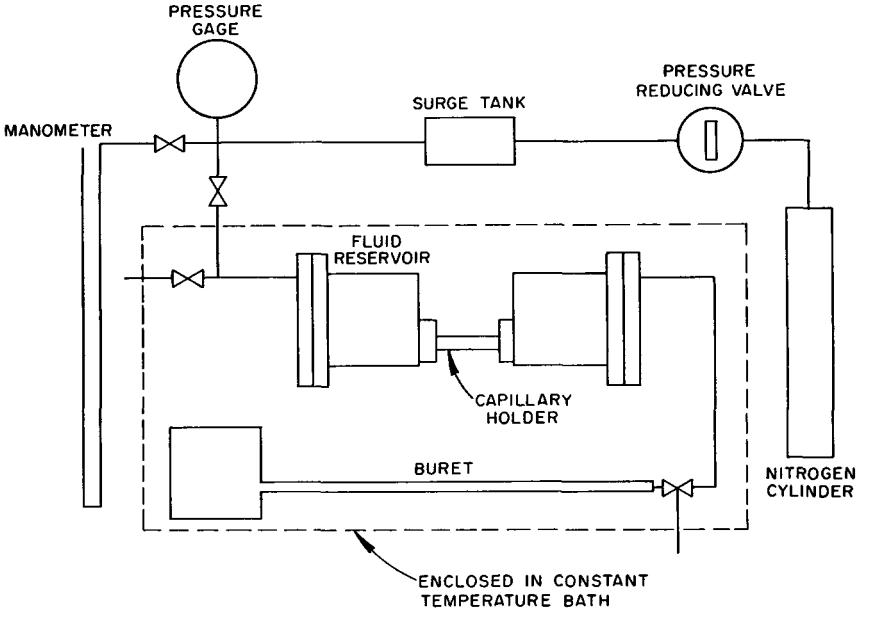

Fig. 2. Schematic diagram of equipment.

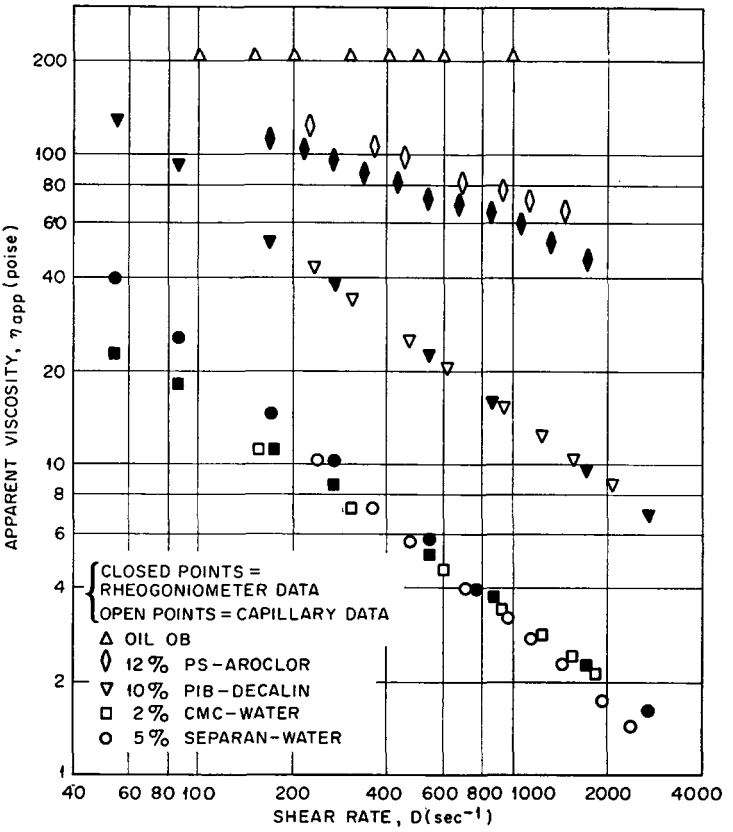

Fig. 3. Apparent viscosities of the test fluids.

0.538 ± 0.001 was bonded with an epoxy cement inside a brass holder. The glass was flush with the entrance, forming a smooth 180° entrance with a diameter ratio of better than 50:1. For the shorter tubes the exit was flush into the brass holder of $^1/_2$ in. inside diameter, with a diameter ratio of 1:10. The total pressure drop was corrected for the exit flow in the $^1/_2$ in. tube. The pressure drop was not affected when the flow direction in the tube was reversed. Most runs were made with exit flow into stagnant test fluid; however, runs were made exiting into air with no significant difference in pressure drop noticeable.

The following polymer solutions were studied: 12% polystyrene (PS) in Aroclor, 10% polyisobutylene (PIB) in decalin, 5% Separan AT 30 (Dow Chemical Company) in water, and 2% carboxymethyl cellulose (CMC) in water. National Bureau of Standards viscosity test oil OB (214.9 poise) was used for testing the calibration of the viscometer.

For the same polymer solutions the primary normal stress difference and shear stress were measured as a function of shear rate on the Weissenberg Rheogoniometer.[32]

ANALYSIS OF DATA

Viscous Behavior

The fluid behavior during developed tube flow was characterized for the Newtonian fluid by the viscosity and for the polymer solutions by the apparent viscosity defined by

$$\eta_{app} = T_{12}/D \tag{14}$$

The results of the developed flow measurements are compared with the rheogoniometer measurements for each fluid investigated (Fig. 3). The linearity of these log–log plots indicates that a power law may be used for describing the fluid behavior over the shear rate range.

The National Bureau of Standards Oil OB was used for checking the calibration of both instruments. From Figure 3 it can be seen that the vis-

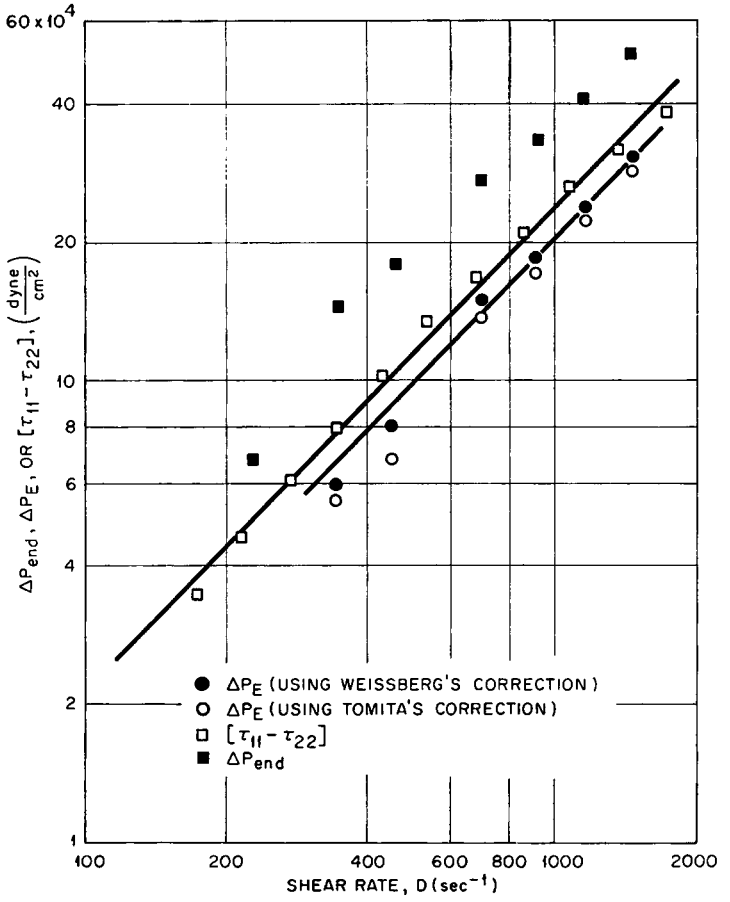

Fig 4. Elastic pressure drop and normal stress difference for the 12% PS–Aroclor solution.

cosity measured by the capillary instrument agreed to within 1.5% of the value provided by the NBS.

The experiments with Oil OB gave some useful data for evaluating the Newtonian analyses for the end-effects pressure loss. The measured values of this pressure loss, from extrapolation of the linear plot of ΔP_{tot} versus L/R to zero length, are presented, with the values predicted by Weissberg's analysis at several shear rates, in Table II. The close agreement over the shear rate range is obvious.

TABLE II
Newtonian Viscous End Effects, NBS Oil OB, Lot 34
$\eta_{25°} = 214.9$ poise

Shear rate, sec.$^{-1}$	η measured, poise	ΔP_{end} measured, psi	ΔP_{end} Weissberg, psi
1000	217.0	6.5	7.4
600	211.0	4.4	4.3
500	211.8	3.2	3.6
400	212.0	2.5	2.9
300	212.0	1.9	2.2
200	216.0	1.5	1.5
150	212.0	1.0	1.1
100	215.9	0.7	0.73

Viscoelastic Behavior

The pressure losses due to end effects for each of the polymer solutions were extracted from the plots of ΔP_{tot} versus L/R and are presented in Figures 4–7 as a function of shear rate. The viscous portions of the pressure drop were approximated with Weissberg's and Tomita's viscous analyses. The difference between the measured total and estimated viscous end-effects losses was assumed to be the loss due to elasticity.

Included in these figures is the plot of normal stress difference $T_{11} - T_{22}$ as a function of shear rate as measured with the rheogoniometer. The linearity of the log-normal stress plots indicates that a power law of the form

$$T_{11} - T_{22} = H_{ch}\lambda_{ch}^{2m}D^{2m} \tag{15}$$

may be used for describing the relationship between primary normal stress difference and shear rate. Equation (3) together with eq. (15) define the material parameters H_{ch} and λ_{ch}.

Examination of Figures 4–7 shows that for a given fluid the slope of the elastic pressure loss (with Weissberg's viscous analysis) versus shear rate is the same as the slope of the normal stress difference versus shear rate. This relationship may be summarized as

$$\Delta P_E = \alpha_3(T_{11} - T_{22}) \tag{16}$$

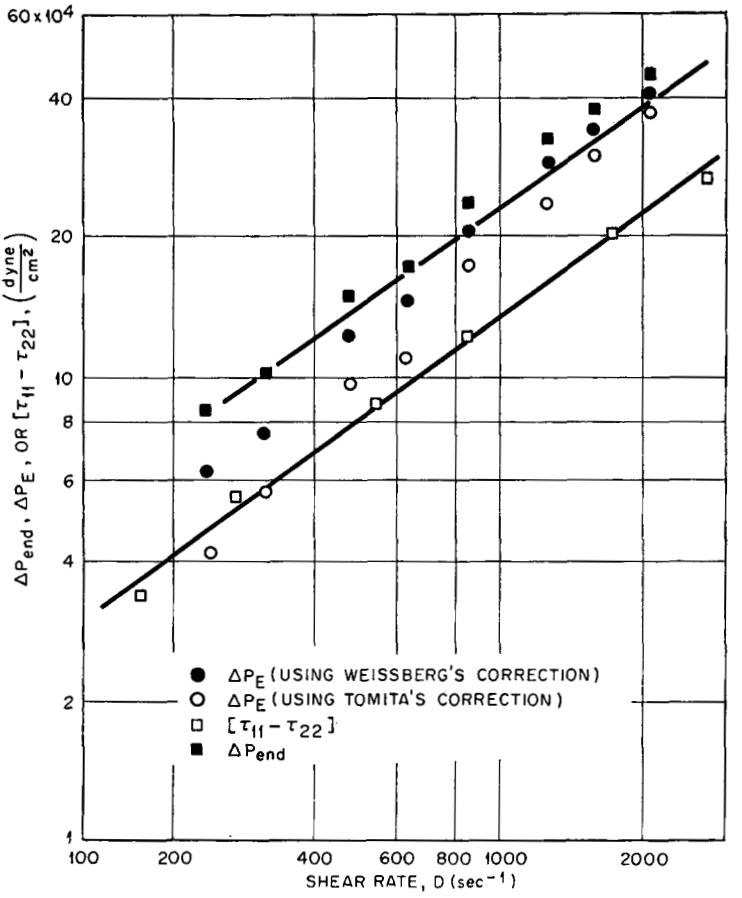

Fig. 5. Elastic pressure drop and normal stress difference for the 10% PIB–decalin solution.

where α_3 is a proportionality constant that depends on the entrance geometry and the fluid.

The experimental results may be summarized in terms of the dimensional analysis equation (eq. 13). The first term of the equation represents the viscous portion of the pressure drop, α_2 being evaluated from Weissberg's (or Tomita's) analysis. The exponent b_2 will either be unity, in Weissberg's analysis, or n, in a power-law analysis. In the elastic term α_3 has been evaluated empirically for the test fluids from Figures 4–7. The exponent b_3 is simply the slope of log-normal stress versus log shear rate.

The material parameters for the test fluids are summarized in Table III. The range in the experimental evaluation of α_3 is due to doubt in the estimation of the viscous portion of the end-effects pressure loss. The fact that the exponent of the relationship for ΔP_E versus shear rate with Weissberg's viscous analysis was so nearly equal to the normal stress power-law

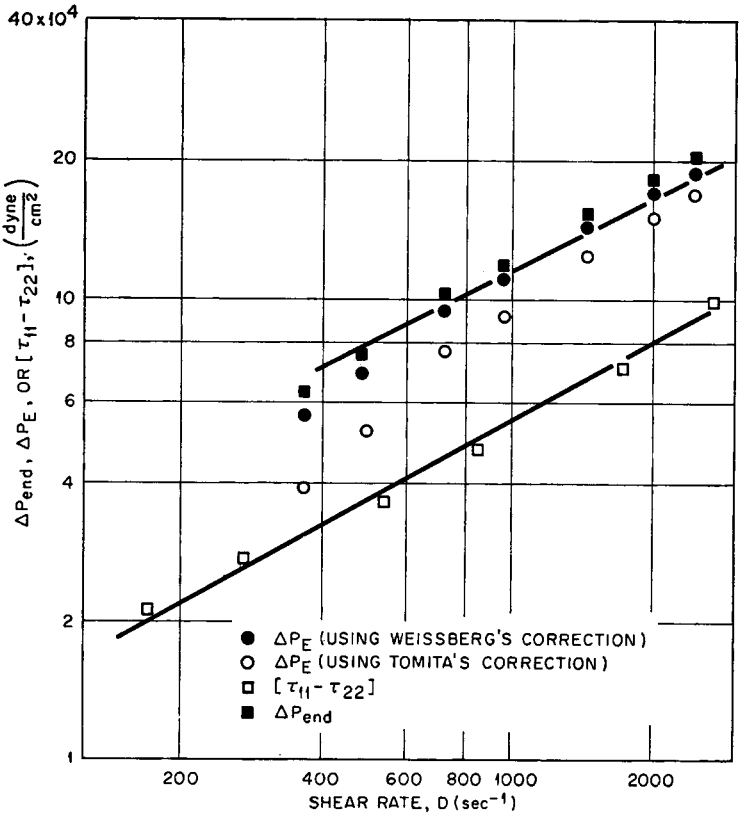

Fig. 6. Elastic pressure drop and normal stress difference for the 5% Separan–water solution.

exponent indicates, however, that his analysis was not a bad approximation for the viscous portion.

A strong correlation was found between the end-effects coefficient α_3 and the elastic power-law exponent m, as can be seen in Figure 8. There was no correlation between α_3 and the viscous power-law exponent n, indicating that the influence of n on the flow field is of secondary importance in the evaluation of the elastic pressure loss.

TABLE III
Viscoelastic Fluid Parameters

Fluid	$2m$	n	$H_{ch}\lambda_{ch}^{n}$ [a]	$H_{ch}\lambda_{ch}^{2m}$ [b]	α_3 (exptl.)
12% PS–Aroclor	1.06	0.64	855	170	0.9 ± 0.2
10% PIB–decalin	0.74	0.30	1950	815	1.7 ± 0.4
5% Separan–water	0.56	0.15	1050	1170	2.1 ± 0.4
2% CMC–water	0.44	0.31	352	500	5.6 ± 0.6

[a] In units of dyne-sec.^{n}/cm.^{2}.
[b] In units of dyne-sec.^{2m}/cm.^{2}.

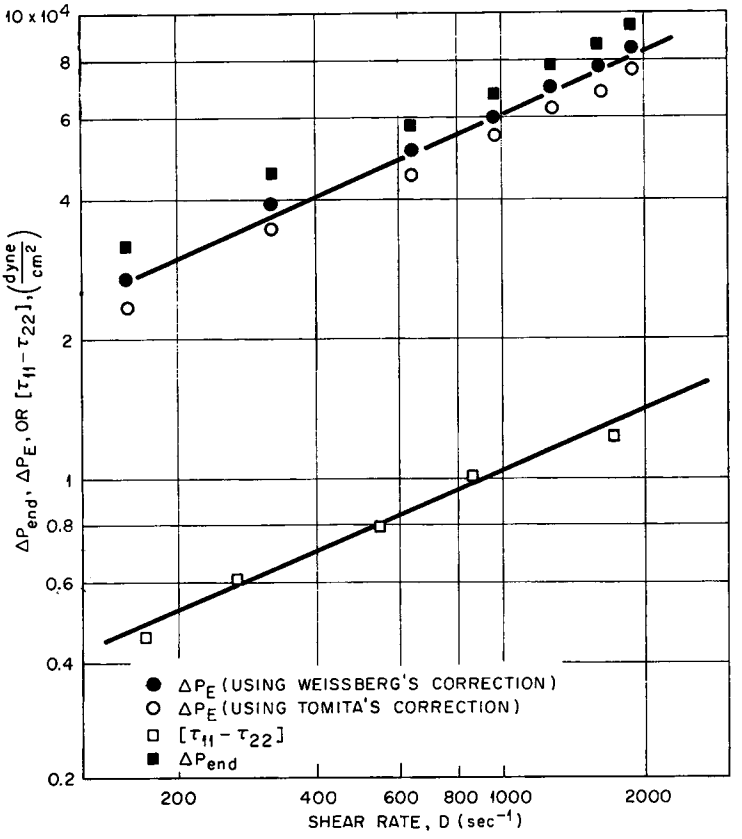

Fig. 7. Elastic pressure drop and normal stress difference for the 2% CMC–water solution.

To explain this correlation of α_3 and, hence, elastic end-effects pressure loss with m, the entrance storing of elastic energy will be considered on the assumption that most of the elastic energy that is stored during the flow is irreversibly dissipated, resulting in the elastic pressure drop. It is important to remember that the elastic entrance pressure drop has been characterized by the wall shear rate in the capillary. Throughout the flow field of interest, the converging flow before the entrance, there is actually a spectrum of shear rates, all lower than the characterizing tube shear rate. The elastic entrance pressure drop might then be visualized as a sum of incremental pressure losses over this flow field, each with its characteristic shear rate between zero and the tube shear rate. Since the normal stress difference is specified explicitly by the shear rate, each of the increments of the elastic entrance pressure loss has its own characteristic normal stress difference. This normal stress difference describes the property of the fluid that causes the elastic entrance pressure loss.

For a fluid with $m = 1$ the normal stress difference is very dependent on shear rate. Very near the entrance, where the shear rate is highest, the

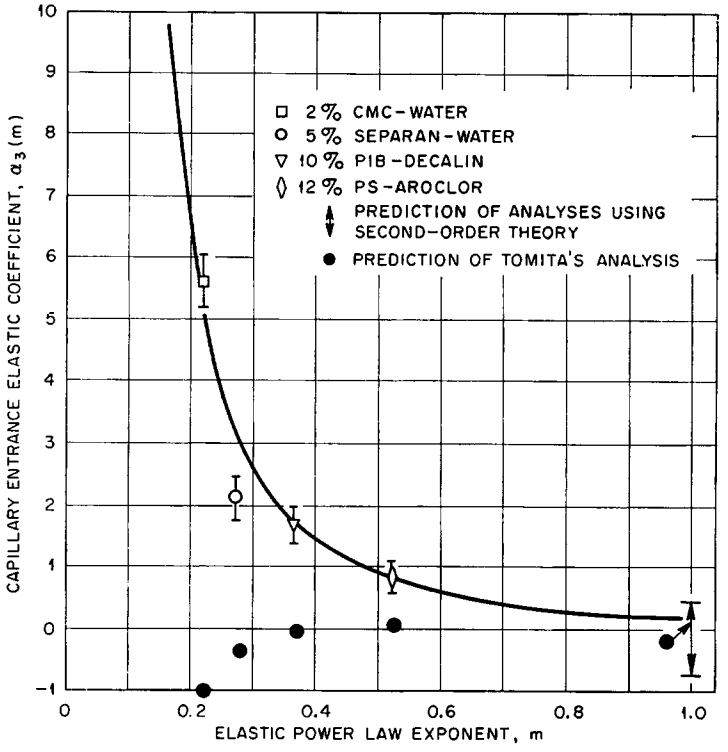

Fig. 8. Elastic coefficient as a function of the elastic exponent m.

normal stress difference would be much greater than at some point farther from the entrance. In this case the incremental elastic pressure losses, which appear to be proportional to the local normal stress difference, would be significant only very near the entrance. For fluids with smaller values of m the normal stress difference would be far less sensitive to shear rate and would have proportionately a much higher value farther upstream from the entrance. The sum of the elastic pressure increments would then have significant terms much farther from the entrance, resulting in a larger total entrance elastic pressure drop.

The experimental results in the form of the dimensional analysis equation (13) are convenient for comparison with the predictions of the theories summarized in Table I. From the large effect of m on α_3 observed it seems that a theory that limits the value of m to unity, as does the second-order theory, cannot correctly relate the end-effects pressure loss to fluid parameters. However, such an analysis might predict the limiting value for the end effects at low flows, where fluids may be described by the second-order theory.

The range of the second-order theory predictions of α_3 is shown in Figure 8. The predicted values were very sensitive to the assumed flow lines and the assumed relationship between the material parameters β and γ. Depend-

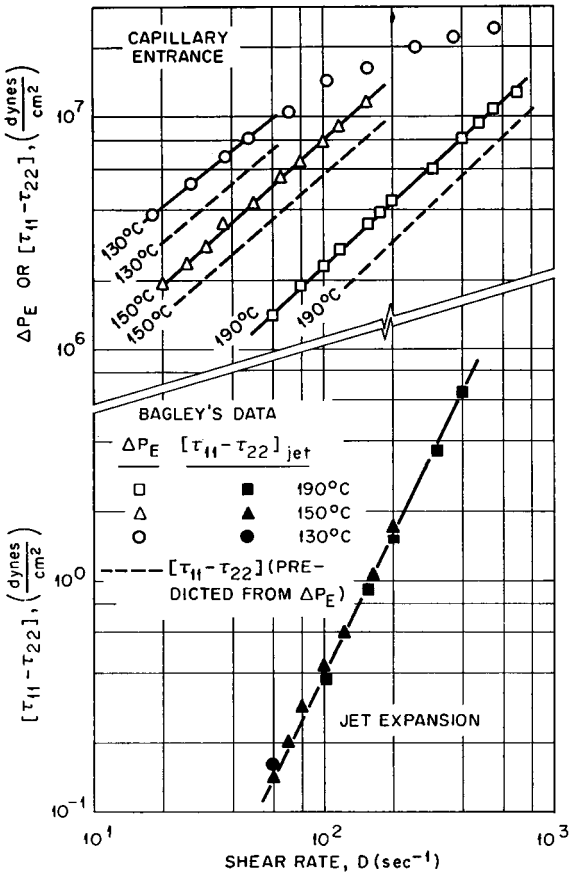

Fig. 9. Comparison of normal stresses calculated by two means for polyethylene melts.

ing on these assumptions, the second-order theory predicts from a small positive to a small negative value of α_3. Extrapolation of the experimental plot of α_3 to $m = 1$, although approximate, does suggest a small positive value of α_3 in agreement with this analysis. Although the Bagley analysis has been the most generally used method for handling the end-effects problem, it has been ineffective when applied to fluids that do not follow "Hooke's law." The requirement that n be equal to m (Hooke's law) limits the applicability of the Bagley method, since n and m differed by more than 50% for some fluids (see Table III). The explicit specification of $\alpha_3 = 1$ further limits the applicability of this method, since Figure 8 shows α_3 to vary from less than 1 to greater than 10, depending on the fluid parameter m. This specified value of α_3 could then result in an order-of-magnitude error in the prediction of the elastic pressure loss for some fluids.

As can be seen from Table I, Tomita's analysis in terms of the entrance pressure drop is of the same form as the equation describing the results of this investigation. It must be remembered that in this comparison

Tomita's small strain fluid parameters have been assumed equivalent to the corresponding flow parameters. With this assumption K_E was evaluated for the fluids of interest.[18] These values were included in Figure 8. As can be seen, Tomita's analysis predicted a reasonable value for a fluid with $n = m = 1$, but the predicted values were too low for all of the test fluids. From this figure it is clear that this analysis does not have the ability needed to predict the effect of m on the elastic pressure drop. Tomita's analysis seems also to be very sensitive to the assumed flow lines. It must be concluded that, although Tomita's analysis predicts the correct form for correlating the end effects, it cannot quantitatively predict them.

Any analysis made to predict accurately the capillary end effects for real viscoelastic fluids at "medium" shear rates must be able to account for the shear rate dependence of both the viscous and elastic properties. Since these analyses appear so sensitive to the assumed flow lines, either the solution for the flow lines must be included in the analysis, or better approximations of the flow lines must be made. Important information about the flow lines might be gleaned from photographic studies of the entrance flow.[33]

Although the experimental evidence shows a definite correlation between α_3 and m for the fluids tested (see Fig. 8), it should be expected that for some fluids secondary normal stress effects and the effects of the viscous properties on the velocity profile might significantly affect the value of α_3. The variation of α_3 in the second-order analyses with the ratio of β to γ illustrates the role that secondary normal stress effects could play. The possible effect of the viscous properties on α_3 is demonstrated in Tomita's analysis, where K_E is shown to be very dependent on n.

An attempt was made to broaden the data to include a polymer melt. Bagley[34] donated capillary data for several polyethylene melts, and jet expansion data that had been taken simultaneously. The results of analysis of the capillary data are presented in Figure 9 with the prediction of the normal stress difference from the correlation between α_3 and m of Figure 8.

A Metzner type of jet analysis[35–37] was used for relating the expansion to normal stresses; however, this method predicted unreasonably low normal stresses and a much stronger shear rate dependence than expected (see Fig. 9). Certain difficulties, notably solidification of the molten jet and short L/R ratios (about 30), complicate the conclusions. However, the gross discrepancies in Figure 9 certainly suggest a "first-order" difficulty in some analysis. Unfortunately, rheogoniometer data are not available for this fluid. Savins[38] noted a similar discrepancy between the jet expansion analysis and the capillary entrance analysis for the concentrated CMC solution data of McIntosh.[39]

CONCLUSIONS

For the polymeric solutions investigated it was possible to correlate over a tenfold shear rate range the elastic pressure drop ΔP_E from the capillary

experiment with the normal stress difference $T_{11} - T_{22}$ from an independent measurement. Both these quantities were similar functions of shear rate (i.e., could be described by the same power-law exponent) and, therefore, were simply proportionally related. The proportionality constant was found to be a strong function of the elastic power-law exponent, a fluid parameter.

A dimensional analysis of the pressure loss due to viscoelastic end effects provided a form of correlating experimental data and of comparing the various analyses of the problem. None of the present analyses were able to predict the large measured dependence of elastic pressure loss–normal stress difference proportionality constant on the elastic power-law exponent. It is apparent that a theory capable of describing highly shear dependent behavior will be necessary.

Finally, gross discrepancies between normal stresses predicted by the capillary entrance method and those predicted by the jet expansion method were noted in polyethylene melts.

The authors wish to thank the National Aeronautics and Space Administration for its support of the final phases of the work under NsG 671. They particularly wish to thank E. B. Bagley and Canadian Industries Limited for providing the polyethylene melt data.

References

1. B. D. Coleman, H. Markovitz, and W. Noll, *Viscometric Flows of Non-Newtonian Fluids*, Springer, Verlag, New York, 1966.
2. B. Bernstein, E. A. Kearsley, and L. J. Zapas, *J. Res. Natl. Bur. Std. B*, **68,**, No. 3, 103 (1964).
3. C. Truesdell and R. Toupin, *Handbuch der Physik*, Vol. III, Pt. 1, Springer-Verlag, Berlin, 1960, pp. 615–647.
4. H. L. La Nieve, III, M.S. thesis, Univ. of Tennessee, Knoxville, 1963.
5. R. B. Bird, W. E. Stewart, and E. N. Lightfoot, *Transport Phenomena*, Wiley, New York, 1960.
6. W. L. Wilkinson, *Non-Newtonian Fluids*, Pergamon, New York, 1960.
7. J. V. Boussinesq, *Compt. Rend.*, **113**, 9 (1891).
8. M. Collins and W. R. Schowalter, *A.I.Ch.E. J.*, **9**, 804 (1963).
9. S. Goldstein, *Modern Developments in Fluid Dynamics*, Vol. 1, Oxford Press, London, 1938.
10. H. L. Langhaar, *J. Appl. Mech.*, **9**, A55 (1942).
11. L. Schiller, *Z. Angew. Math. Mech.*, **2**, 94 (1922).
12. D. C. Bogud, *Ind. Eng. Chem.*, **51**, 874 (1959).
13. Y. Tomita, *Bull. JSME*, **4**, 77 (1961).
14. Y. Tomita, *Chem. Engr. Japan*, **23**, 525 (1959).
15. A. B. Metzner and J. L. White, *A.I.Ch.E. J.*, **11**, 989 (1965).
16. H. L. Weissberg, *Physics of Fluids*, **5**, 1033 (1962).
17. Y. Tomita, *Trans. JSME*, **25**, 938 (1959).
18. H. L. La Nieve, III, Ph.D. thesis, Univ. of Tennessee, Knoxville, 1966.
19. W. Philippoff and F. H. Gaskins, *Trans. Soc. Rheol.*, **2**, 263 (1958).
20. E. B. Bagley, *Trans. Soc. Rheol.*, **5**, 355 (1961).
21. Y. Tomita, *Bull. JSME*, **5**, 443 (1962).
22. D. C. Bogue and J. O. Doughty, "Comparison of constitutive equations for viscoelastic fluids," paper presented to A.I.Ch.E. (Dec. 1965).
23. E. B. Adams, J. C. Whitehead, and D. C. Bogue, *A.I.Ch.E. J.*, **11**, 1026 (1965).

24. B. D. Coleman and H. Markovitz, *J. Appl. Phys.*, **35**, 1 (1964).
25. S. Oka, *J. Phys. Soc. Japan*, **19**, 1481 (1964).
26. K. Weissenberg, *Nature*, **159**, 310 (1947).
27. H. Markovitz, *Proc. 4th Intern. Cong. Rheol.*, Part 1, Brown Univ., Providence, R. I., 1963, pp. 189–212.
28. H. Markovitz and D. R. Brown, *Trans. Soc. Rheol.*, **7**, 137 (1963).
29. T. Arai and H. Aoyama, *Trans. Soc. Rheol.*, **7**, 333 (1963).
30. E. B. Bagley, *J. Appl. Phys.*, **28**, 624 (1957).
31. Y. Tomita and K. Tsuchiya, *Bull. JSME*, **6**, 709 (1963).
32. J. O. Doughty, Ph.D. thesis, Univ. of Tennessee, Knoxville, 1966.
33. M. J. Vignale, *J. Polymer Sci. B*, **2**, 799 (1965).
34. E. B. Bagley, unpublished experimental data, Canadian Industries Limited, McMasterville, Quebec, 1961.
35. A. B. Metzner, E. L. Carley, and S. K. Park, *Mod. Plastics*, **37**, 133 (1960).
36. A. B. Metzner, W. T. Houghton, R. E. Hurd, and C. C. Wolfe, paper presented at Conference of Second-Order Effects in Elasticity, Plasticity, and Fluid Dynamics, Haifa, Israel, 1964, pp. 650–668
37. A. B. Metzner, W. T. Houghton, R. A. Sailor, and J. L. White, *Trans. Soc. Rheol.*, **5**, 133 (1961).
38. J. G. Savins, *J. Appl. Polymer Sci.*, **6**, 567 (1962).
39. D. L. McIntosh, Sc.D. thesis, Washington Univ., St. Louis, Mo., 1960.

Received January 23 1967